Site-Specific Phosphorylation of Human p53 Protein Determined by Mass Spectrometry†

B. Alex Merrick,‡ Wei Zhou,§ Karla J. Martin,‡ Shanthini Jeyarajah,§ Carol E. Parker,§ James K. Selkirk,‡ Kenneth B. Tomer,§ and Christoph H. Borchers*,§

Laboratory of Molecular Carcinogenesis and Laboratory of Structural Biology, National Institute of Environmental Health Sciences, Research Triangle Park, North Carolina 27709

Received August 29, 2000; Revised Manuscript Received December 7, 2000

ABSTRACT: Human recombinant p53 (r-p53) protein was studied by mass spectrometry (MS) to determine site-specific posttranslational differences between basal and hyperphosphorylated r-p53. Wild-type p53 was basally expressed after baculovirus infection while a parallel preparation was treated with the phosphatase inhibitor okadaic acid during the terminal stages of expression to create a hyperphosphorylated form of p53 known for its higher DNA binding and transcriptional activation. After immunoaffinity and HPLC purification, MALDI/MS measured a higher molecular mass for r-p53 from okadaic acid treatment relative to control, suggesting a higher phosphorylation state. This was supported by an acidic shift of r-p53 isoforms separated by gel isoelectric focusing. Employing a variety of mass spectrometric analyses combined with separation and affinity techniques, six specific phosphorylation sites of p53 were identified. The MS data indicated that hyperphosphorylated p53 showed a higher degree of phosphorylation than basal p53 at specific amino- and carboxy-terminal sites. In particular, ESI-MS demonstrated that Ser^{315} was entirely phosphorylated after okadaic acid treatment, as confirmed biochemically by CDK2 kinase assay and by isoelectric focusing. In summary, MS analysis uniquely revealed increased, site-specific phosphorylations on p53 after phosphatase inhibition, particularly at Ser^{315}, which may be critical molecular events in defining p53 activity.

Phosphorylation and acetylation of the p53 protein are intimately involved in signal integration and cellular response to specific types of stress (*1, 2*). DNA damage, topoisomerase II inhibitors, or JNK/MEKK[1] pathway activation can initiate amino-terminal phosphorylation of human p53 that is associated with mdm2 and JNK release and stabilization of p53 (*3*−*7*). Release of mdm2 and JNK from p53 interrupts ubiquitin−proteosomal degradation and stabilizes p53 levels (*6, 8*−*10*). Phosphorylation of p53 at Ser^{15}, Thr^{18}, and Ser^{20} has been particularly associated with release of mdm2 by several kinases, including DNA PK (*3*), ATM (*5*), ATR (*11*), Chk2/hcds 1 (*12*), and CK1 δ (*13*). Prior phosphorylation of mdm2 itself via ATM may also be involved prior to mdm2 release from p53 (*14*). Dissociation of the p53−mdm2 complex may also be assisted by Ser^{33} and Ser^{37} phosphorylation from DNA PK (*15*), ATR (*16*), and CDK7−cyclin H−p36MAT1 complex (*17*) kinases. Acetylation of lysine residues at the carboxy terminus of p53 at Lys^{373} and Lys^{382} by p300/CBP and at Lys^{320} by PCAF, possibly recruited by phosphorylation at Ser^{33} and Ser^{37} as well as Ser^{15}, imparts higher transcriptional activity to p53 (*2, 18*). At the C-terminal domain of p53, enhancement of sequence-specific DNA binding occurs by phosphorylation of the p53 C-terminal regulatory domain by several kinases including CDK2/cdc2 kinases at Ser^{315}, PKC at Ser^{371}, Ser^{376}, and Ser^{378}, and CKII or PKR at Ser^{392} (*19*−*22*).

Recent studies show that interdependent and sequential modifications of p53 also influence its activity. For example, ionizing irradiation leads to dephosphorylation of the PKC site, Ser^{376}, enhanced binding of 14-3-3 proteins, and subsequent transcriptional activation (*23*). Low-level UV

† A preliminary report of this study was first presented at the American Association of Mass Spectrometry Meeting in Dallas, TX, on June 8−11, 1999, by Borchers, C., Parker, C. E., Mueller, K., Zhou, W., Merrick, B. A., Jeyarajah, S., and Tomer, K. B., "Determination of the phosphorylation sites on p53, a tumor suppressor protein".

* Correspondence should be addressed to this author at the Laboratory of Structural Biology, MD: F0-04, National Institute of Environmental Health Sciences, 111 Alexander Dr., Research Triangle Park, NC 27709. Phone: (919) 541-5108, Fax: (919) 541-0220, Email: borchers@niehs.nih.gov.

‡ Laboratory of Molecular Carcinogenesis .

§ Laboratory of Structural Biology.

[1] Abbreviations: JNK, c-jun-N-terminal kinase; MEKK, mitogen-activated protein kinase kinase; CDK, cyclin-dependent kinase; mdm2, murine-double-minute-2; Ser, serine; Lys, lysine; DNA PK, DNA protein kinase; ATM, ataxia−telangectasia mutated; ATR, AT Rad3-related; Chk2, checkpoint kinase-2; CK1, creatine kinase-1; MAT1, menage a trois 1; CRB, CREB binding protein; PCAF, p300/CBP-associated factor; PKR, RNA-activated protein kinase; PKC, protein kinase C; UV, ultraviolet; MS, mass spectrometry; MALDI, matrix-assisted laser desorption ionization; OA, okadaic acid; r-p53, recombinant p53; wt, wild type; DMSO, dimethyl sulfoxide; MOI, multiplicity of infection; EDTA, ethylenediaminetetraacetic acid; NP-40, Nonidet P-40; LiCl, lithium chloride; DTT, dithiothreitol; PIPES, piperazine-*N*,*N*′-bis(2-ethanesulfonic acid); LC, liquid chromatography; HPLC, high-pressure liquid chromatography; IMAC, immobilized metal affinity chromatography; HEPES, *N*-(2-hydroxethyl)piperazine-*N*′-2-ethanesulfonic acid; Da, dalton(s); ESI, electrospray ionization; MS/MS, tandem mass spectrometry; aa, amino acid(s); Asp-N, endoprotease Asp-N; PPA, protein phosphatase A; 2D PAGE, two-dimensional polyacrylamide gel electrophoresis; SDS−PAGE, sodium dodecyl sulfate−polyacrylamide gel electrophoresis; IEF, isoelectric focusing; Ga, gallium.

10.1021/bi002045i CCC: $20.00
Published on Web 02/20/2001

radiation leads to dephosphorylation of Ser^{20} in A375 cells and increased steady-state phosphorylation at Ser^{392} without p53 protein stabilization (*24*). In MCF-7 cells, stress-activated p38 kinase phosphorylates p53 on Ser^{33} and possibly on a newly discovered site, Ser^{46}, as a prerequisite for normal UV-induced phosphorylation at Ser^{37} and Ser^{15} (*25*). Dual phosphorylation of p53 at Ser^{15} and Ser^{392} was required for activation since Ser^{15-P} inhibited mdm2 binding and Ser^{392-P} induced DNA binding of p53 (*26*). Thus, multisite phosphorylation as well as dephosphorylation and acetylation events apparently participate in the formation of activated p53 subpopulations, free from mdm2 or JNK inhibition and capable of selective binding to specific gene promoter regions or to members of the transcriptional apparatus.

Identification of specific phosphorylation sites on p53 and direct linkage to p53-mediated effects *in vivo* have historically not been very straightforward. Site-specific determination of phosphorylation often involves phosphopeptide mapping with radionuclides. However, the process of cellular labeling with ortho[^{32}P]phosphate and [^{35}S]methionine in human diploid fibroblasts actually induces p53 protein expression by 3−4-fold compared to control, alters p53 immunoreactivity, and produces growth arrest (*27*). Such DNA-damaging effects of radionuclides may upregulate the basal level of phosphorylation and kinase activity of many cell types. The interdependency of phosphorylation sites for p53 action has made studies with single- and multi-site-directed mutagenesis of phosphorylation sites on p53 difficult to interpret (*28*, *29*). However, the introduction of phospho-specific antibodies raised to specific phosphoserine, phosphothreonine, and acetylated lysine residues in p53 has provided new sensitive reagents to study posttranslational modifications to p53 in a nondisruptive manner compared to radioisotopes. While many recent advances have come about with these new site-specific immunoreagents, there are some potential shortcomings, including reliance upon "known" sites, an inability to detect posttranslational changes involving "dephosphorylation", and exclusion of other potentially important modifications such as ribosylation (*30*, *31*), O-glycosylation (*32*), or SUMO-1 addition (*33*) as reported in specific cell types.

Sophisticated methods for measuring the fine structure of p53 by mass spectrometric (MS) analysis could be helpful in relating protein phosphorylation to biological activity. Recent studies have demonstrated the power of MS analysis in relating the structural biology of the human p53 molecule to its tumor suppressor effects (*2*). In one report, ultraviolet and ionizing radiation activated a signal transduction pathway which increased phosphorylation of Ser^{33} and Ser^{37} on p53 protein as determined by nanospray ion trap MS of trypsin digestion fragments. These modifications enhanced the affinity of specific histone acetylases for p53 at Lys^{320} and Lys^{382}, resulting in increased sequence-specific DNA binding and transactivation activity of the modified p53 protein. Another study used MALDI/MS following tryptic digestion to verify the presence of phosphate groups on Ser^{375} and Ser^{392} of p53 in characterizing the epitope for a new monoclonal antibody recognizing phosphorylated p53 (*34*). Other studies have used MALDI/MS and tandem MS to confirm the identity of p53 peptides (*35*) or to perform direct DNA sequencing of the p53 gene for mutation analysis (*36*−*38*).

We have previously reported that human p53 protein could be resolved into phosphoisoforms by isoelectric focusing (*39*, *40*). The comparable pattern of p53 phosphoisoforms that can be resolved from baculovirus expression and primary human cells (*40*) suggested to us that the posttranslational processes in sf9 cells could model phosphorylation of p53 from human cells. Others have reported that the basal level of p53 phosphorylation both *in vivo* (*41*, *42*) and in baculovirus expression systems (*43*) could be greatly increased by the phosphatase inhibitor, okadaic acid. Hyperphosphorylated p53 from okadaic acid treatment may mimic some activated forms of p53 as measured by *in vitro* DNA binding assays showing increased binding to the p53 consensus sequence and RGC motifs as well as reduced binding to the p53 response element of the bax1 gene promoter (*37*, *43*). We wanted to explore the phosphorylation state of p53 without the biologic perturbations experienced during peptide mapping with radionuclides. The purpose of our study was to compare site-specific phosphorylation in the basal and hyperphosphorylated forms of baculovirus r-p53 by mass spectrometric analysis combined with a variety of chromatographic separation techniques.

MATERIALS AND METHODS

Expression of Human r-p53. Sf9 insect cells which had been adapted to suspension culture were maintained in serum-free Grace's complete medium (Sf-900 II SFM, Life Sciences, Gaithersburg, MD). Sf9 cells were grown in sterile Erlenmeyer culture flasks (Corning Inc., Corning, NY) in ambient conditions using a rotary incubator at 135 rpm at 27 °C (Innova 4080, New Brunswick Scientific Co., Edison, NJ). Log-phase growth cultures of sf9 cells were grown to a density of 2×10^6 cells/mL at a viability of >95% by trypan blue exclusion. Volumes of 100 mL sf9 cell suspensions were infected with a titer of 5 MOI of baculovirus containing wild-type human p53 cDNA as previously described (*40*). At 36 h post-infection, sf9 cells were treated with 25 nM of the phosphatase inhibitor, okadaic acid, dissolved in DMSO. Controls received DMSO alone at 0.1% volume. After 48 h, cells from each incubate were harvested.

Immunoaffinity Purification of r-p53. After incubation, r-p53 from sf9 cells was isolated by immunoaffinity chromatography according to (*44*). Briefly, cells from 100 mL of expression culture were washed and solubilized in 4 mL of lysis buffer (150 mM NaCl, 150 mM Tris-HCl, pH 8, 1 mM EDTA, 0.5% NP-40 with protease and phosphatase inhibitors) on ice for 0.5 h. Insoluble material was removed from sf9 cell lysates by centrifugation (SW-50 rotor) at 40 000 rpm for 35 min at 4 °C in a Beckman ultracentifuge. PAb122 anti-p53 antibody obtained from murine ascites fluid was covalently bound to Protein A Sepharose beads (Protein A Sepharose 4 Fast Flow, Amersham Pharmacia Biotech, Piscataway, NJ) using the cross-linking agent dimethyl pimelimidate. A 2.5 mL volume of sf9 lysate was diluted with an equal volume of lysis buffer and was added to 2 mL of packed Sepharose beads bound with anti-p53 antibody. The batch technique was used for binding r-p53 with gentle rotation overnight at 4 °C. Nonspecifically bound proteins were removed by washing beads 5 times each with stripping buffer (50 mM Tris-HCl, pH 8, 0.5 M LiCl, 1 mM EDTA, 10% glycerol), equilibration buffer (10 mM Pipes, 5 mM NaCl, 1 mM EDTA, 10% glycerol), and elution buffer (50

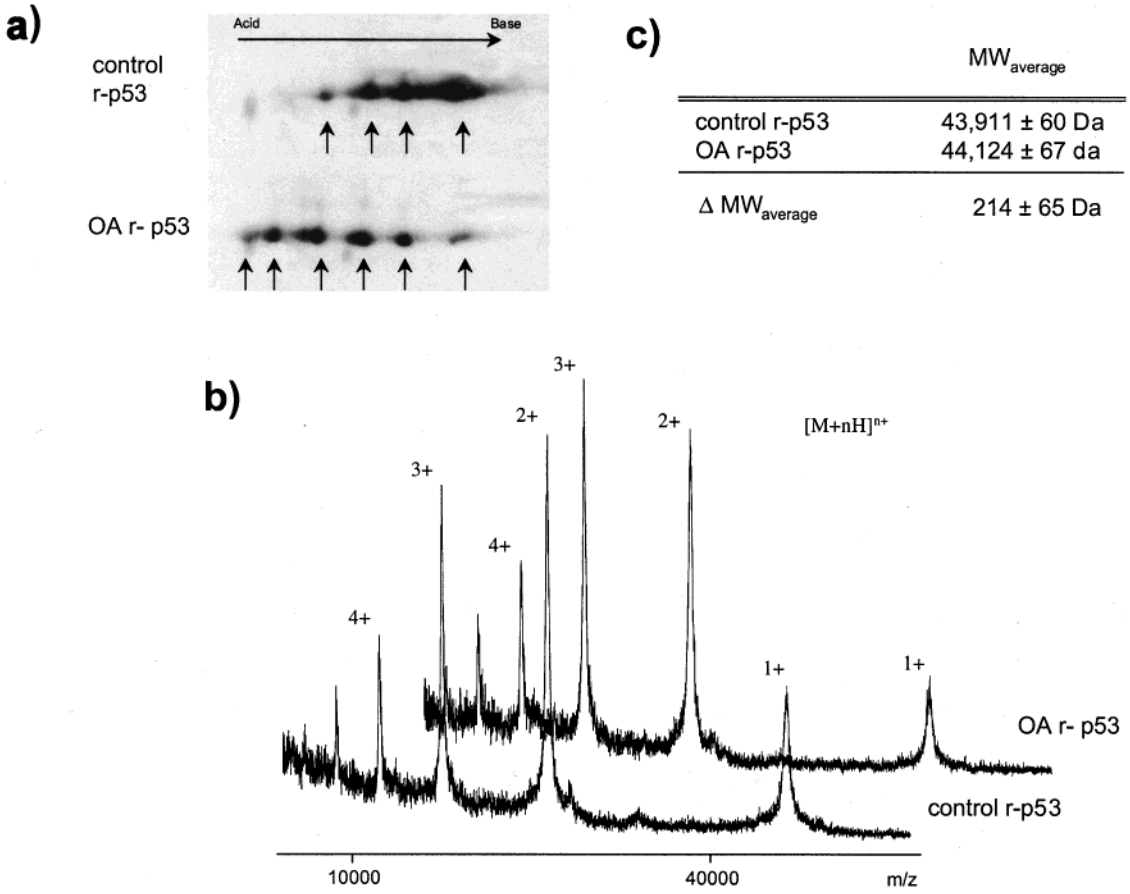

FIGURE 1: Mass spectrometric analysis and electrophoretic separation of human r-p53 isoforms. Human r-p53 was isolated from baculovirus-infected sf9 insect cells which were treated with vehicle (control r-p53) or the phosphatase inhibitor, okadaic acid (OA r-p53), during the final 12 h of a 48 h expression period. After immunoaffinity purification and HPLC separation, these samples were analyzed for mass differences by MALDI/MS or for charge differences by two-dimensional polyacrylamide gel electrophoresis (2D PAGE). Panel a: Western blot of purified human r-p53 from control and OA preparation after 2D PAGE separation. Purified r-p53 was separated electrophoretically by charge (isoelectric focusing) and mass (SDS−PAGE), immunoblotted with anti-p53 antibody, and detected by chemiluminescence. In control p53 expressions, four major isoforms are observed, while in okadaic acid preparations, six isoforms appear which were positionally shifted toward the acidic portion of the isoelectric gradient. The acidic shift in r-p53 isoforms after OA treatment is consistent with hyperphosphorylation of OA r-p53 relative to control r-p53. Panel b: Mass determination by MALDI/MS of purified control r-p53 and OA r-p53. Panel c is a table showing the higher mass of OA r-p53 compared to control r-p53 averaged over 3 spectra.

mM Tris-HCl, pH 8, 150 mM NaCl, 1 mM EDTA, 0.5% NP-40). r-p53 was eluted for 8 h in 5 mL of elution buffer containing 1 mg of the amidated peptide, KKGQSTSSRHK, containing the epitope for the anti-p53 monoclonal antibody, PAb122. A second elution with 0.5 mg of elution peptide for 4 h ensured complete recovery of p53. Elution fractions were combined and dialyzed twice for at least 6 h against a solution of 100 mM Pipes, pH 7, 50 mM NaCl, 1 mM EDTA, 1 mM DTT, and 50% glycerol. Fractions were subaliquoted and frozen at −80 °C until use.

Chromatography. r-p53 was chromatographed to remove glycerol and other interfering ions prior to MS analysis. Liquid chromatography (Hewlett-Packard LC model 1100, Hewlett Packard, Palo Alto, CA) of immunoaffinity-purified r-p53 was performed on a Vydac C-4 column (250 × 4.6 mm, 10 μm particle size; Vydac, Hesperia, CA) using a linear gradient from 9 to 54% acetonitrile containing 0.1% trifluoroacetic acid at a flow rate of 1 mL/min at 25 °C for 50 min. Samples were lyophilized and stored at −80 °C. Separation of tryptic peptides was performed on a Vydac C-18 column using a 9−54% acetonitrile gradient containing 0.1% trifluoroacetic acid (1 mL/min at 25 °C for 50 min). Phosphorylated residues are stable under these chromatographic conditions (*45*).

Immobilized metal affinity chromatography (IMAC) to isolate p53 phosphopeptides was performed according to (*46, 47*). Briefly, nickel-nitrilotriacetic agarose (Ni-NTA, Qiagen Inc., Chatsworth, CA) was stripped of nickel ion with 100 mM EDTA, replaced with gallium ions (60 mM $GaCl_3$), and washed with distilled, deionized H_2O. Binding of r-p53 phosphopeptides to the Ga^{3+} IMAC matrix was carried out by mixing 30 μL of a 50% slurry of the Ga^{3+} matrix in a minicolumn with 2 μg of r-p53 protein digest in a rotating incubator at 37 °C for 30 min. The column was washed with water followed by 0.1 M acetic acid to remove less tightly bound peptides. A 0.5 μL aliquot of the resin was placed directly onto the MALDI target followed by 0.5 μL of matrix solution. The sample was dried at room temperature before MS analysis.

Enzymatic Digestions. HPLC-purified r-p53 (200 μg) was lyophilized and redissolved in 20 μL of 50% acetonitrile. Trypsin (Worthington, NY) at a 1:100 concentration was added together with r-p53 in 80 μL of 50 mM NH_4HCO_3, pH 8, and incubated at 37 °C for 4 h. The Asp-N digestion

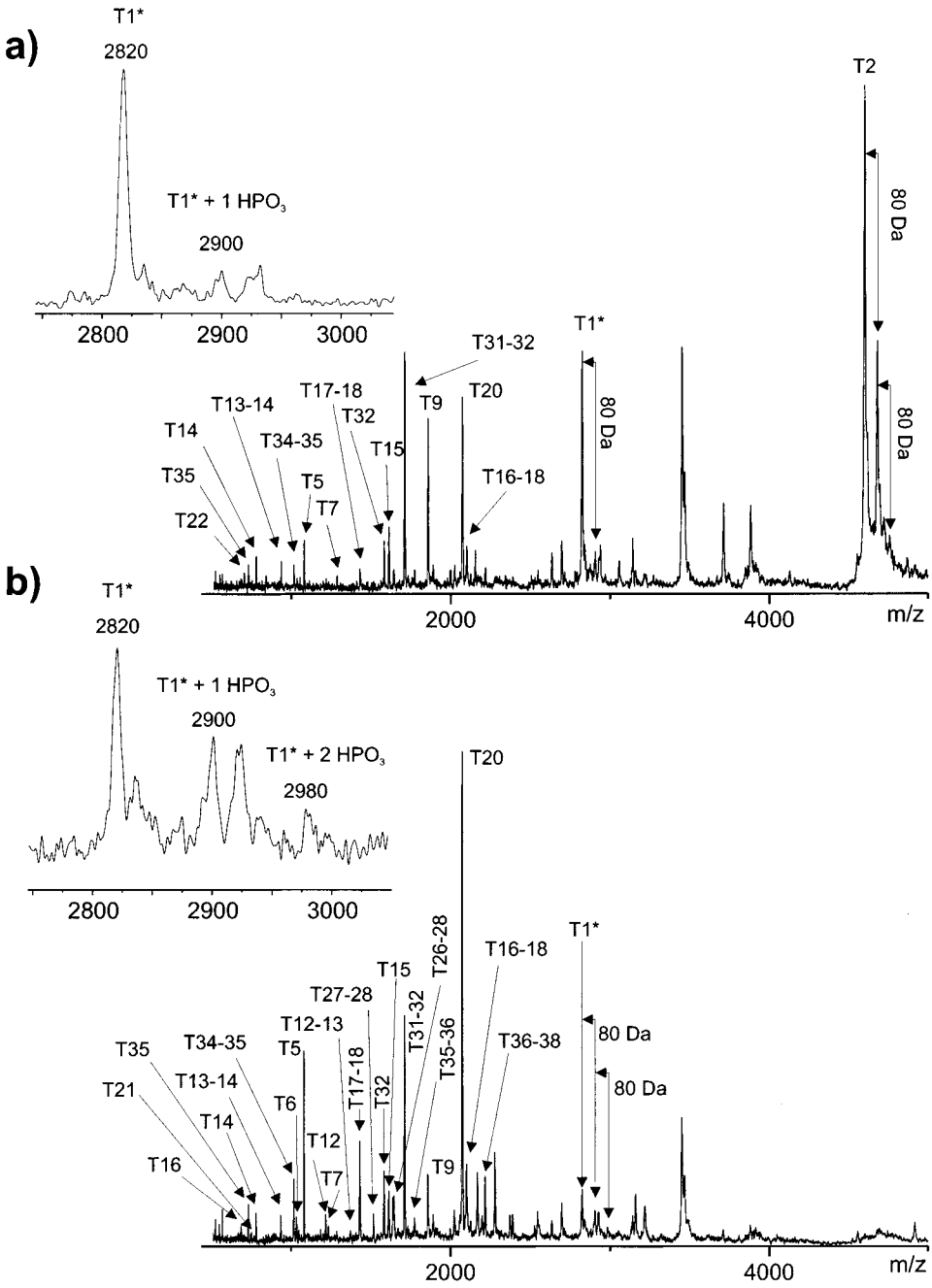

FIGURE 2: Mass spectrum from MALDI/MS of the tryptic digest of control r-p53 (panel a) and OA r-p53 (panel b). Purified r-p53 was digested with trypsin according to Materials and Methods and analyzed by MALDI/MS without further separation. Insets in the upper left portion of each panel show an enlarged portion of the *m*/*z* spectrum for the r-p53$^{1-24}$ T1 peptide that more clearly shows a monophosphorylated species in the control and mono- and diphosphorylated r-p53$^{1-24}$ T1 peptides for okadaic acid treatment.

was carried out on HPLC-separated tryptic peptides of r-p53 which were redissolved as above and incubated with 40 ng of Asp-N enzyme (Roche, Nutley, NJ) in 80 μL of 50 mM NH_4HCO_3, pH 8, at 37 °C for 4 h.

Mass Spectrometry. MALDI/MS analysis was performed on a Voyager-RP time-of-flight mass spectrometry (Perseptive Biosystems, Framingham, MA) in the linear mode with an accelerating voltage of 30 kV and a 1.3 m flight path. A 337 nm nitrogen laser was used to desorb/ionize samples. Samples were prepared for MALDI by the dried-droplet method with a saturated solution of recrystallized α-cyano-4-hydroxycinnamic acid in ethanol/water/formic acid. All electrospray-ionization (ESI) analyses were performed on a Micromass Q-TOF, equipped with a nebulized nanospray electrospray source (nanoflow-ESI/MS). For LC-MS analyses, a Gilson HPLC-system was used with a Hypersil C18 column and Accurate Splitter (LC Packings, San Francisco, CA) at a flow rate of 200−300 nL/min. A water/acetonitrile gradient was used for separation with both mobile phases containing 0.1% formic acid, in which phosphopeptides are stable. Peptides were separated using a 5−95% gradient of acetonitrile at 25 °C.

CDK2 Kinase Assay. CDK2 kinase assay was performed according to (*48*). Briefly, CDK2−cyclin complex was isolated by immunoprecipitation from HT1080 human fibrosarcoma cell lysates at 0.2 mg of cell lysate per kinase reaction. Cells were lysed in an immunoprecipitation buffer (50 mM Tris, pH 8, 130 mM NaCl, 1 mM EDTA, 1% NP-

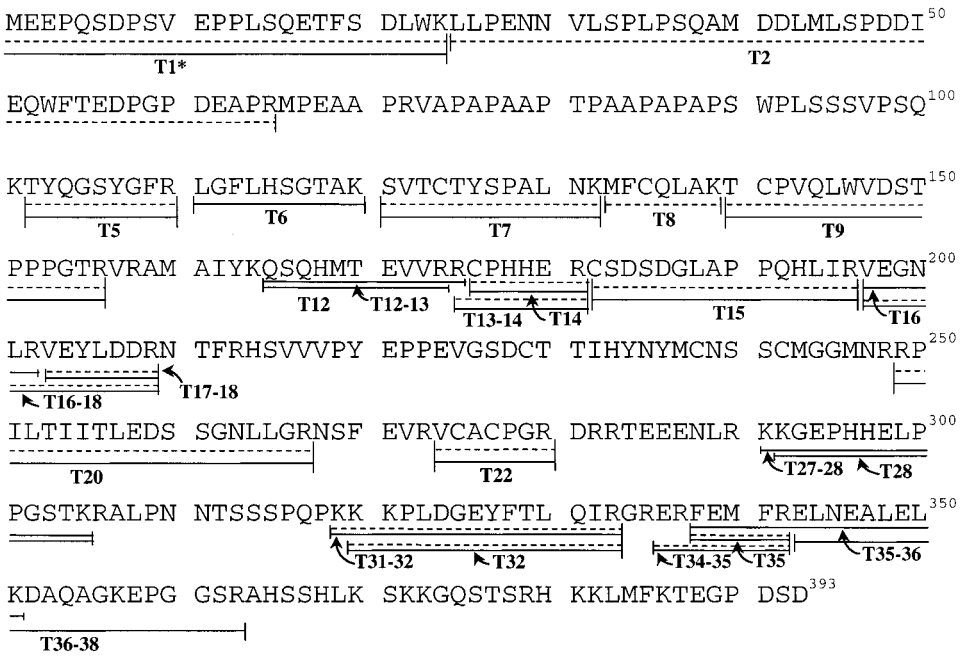

FIGURE 3: Amino acid sequence of human p53 and corresponding tryptic map assembled after MALDI/MS analysis. Annotated dashed horizontal lines were derived from control r-p53 tryptic fragments while solid horizontal lines represent OA r-p53 peptides. Short vertical lines show fragment ends. Tryptic peptides are in numerical order from the amino to the carboxy terminus.

40 with protease) (Protease Inhibitor Cocktail, Roche, Indianapolis, IN) and phosphatase inhibitors, 20 mM NaF, 1 mM β-glyceryl phosphate, and 1 mM *p*-nitrophenyl phosphate. The latter two chemicals served as alternate inorganic and organic substrates for cellular phosphatases, respectively (*47*). Whole cell lysates were created by progressive needle-shearing to fragment DNA. Cell debris was pelleted by centrifugation at 12000*g* for 20 min at 4 °C. Protein concentration of the lysate was determined, and 200 μg of lysate protein was incubated with 2 μg of anti-CDK2 (M-2 antibody; Santa Cruz Biotech., Santa Cruz, CA). Nonspecific kinases were collected using IgG rabbit serum as the primary antibody (Vector, Burlingame, CA). Immune complexes were collected by rotation for 1 h at 4 °C with protein-G agarose beads coated with anti-rabbit IgG (Roche). Beads were washed 4 times with immunoprecipitation buffer and twice with kinase buffer (50 mM HEPES, pH 7.6, 10 mM $MgCl_2$, and 1 mM dithiothreitol). Each immunoprecipitate received 15 μL of kinase buffer also containing 1 mM NaF, 10 mM β-glyceryl phosphate, 200 μM ATP, and 1 μg of r-p53 as substrate. Reactions were conducted at 30 °C for 30 min. Reactions were stopped by addition of 20 μL of 2× lysis buffer (250 mM Tris-HCl, pH 6.8, 1% SDS, 10% glycerol, 20 mM DTT; 0.01% bromophenol blue) for SDS−PAGE.

Separation of p53 Isoforms. Resolution of p53 phosphoisoforms by isoelectric focusing was performed as previously described (*39*, *40*). Briefly, r-p53 was dissolved in urea-based lysis buffer and separated by equilibrium isoelectric focusing using pH 4−8 liquid ampholytes in tube gels. Isoforms were then separated by mass over an 10−16% SDS−PAGE gradient gel. For Western blotting of r-p53 phosphoisoforms, protein was transferred from SDS−PAGE gels to nitrocellulose, probed with PAb122 monoclonal antibody (Roche), and detected by chemiluminescence with an anti-mouse HRP antibody (Roche) as previously described (*40*).

RESULTS

Differential Phosphorylation Status of r-p53 Expressed in the Presence of OA. Wt p53 protein was expressed in the baculovirus system in the absence (control r-p53) or presence (OA r-p53) of the phosphatase inhibitor OA. The first step in the characterization of r-p53 expressed under the two conditions was to determine the number of phosphorylated isoforms by 2D PAGE followed by Western blot for p53 (Figure 1a). The analysis of control r-p53 and of OA r-p53 showed four and six isoforms, respectively. From these observations, we would infer that there are at least four to six phosphorylation sites isolated from this expression system and that the amount of phosphorylation is greater after OA treatment. Immunoaffinity-purified r-p53 proteins were then purified by HPLC prior to mass spectrometric analysis. The MALDI/MS spectra of the HPLC-purified proteins show only ions corresponding to r-p53, indicating high purity for these preparations (Figure 1b). The molecular mass was calculated from the average of the molecular masses of the singly to quadruply charged ions and is shown in Figure 1c as an average of three experiments. The difference of 214 ± 65 Da between the molecular masses of control r-p53 and OA r-p53 corresponds to an additional average incorporation of 2.7 ± 0.8 phosphoryl groups in OA r-p53, assuming that the molecular mass shift is caused only by phosphorylation. This mass spectrometric result is in good agreement with the result obtained by 2D PAGE followed by Western blot analysis. ESI spectra of the two r-p53's were also obtained but were not well enough resolved to provide additional information after deconvolution (data not shown).

The N-Termini of Control r-p53 and OA r-p53 Are Differentially Phosphorylated. To identify the sites of modifications in control r-p53 and OA r-p53, the proteins were digested with trypsin and analyzed by different mass spectrometric techniques in combination with various separation strategies. The first analysis was by MALDI/MS of the

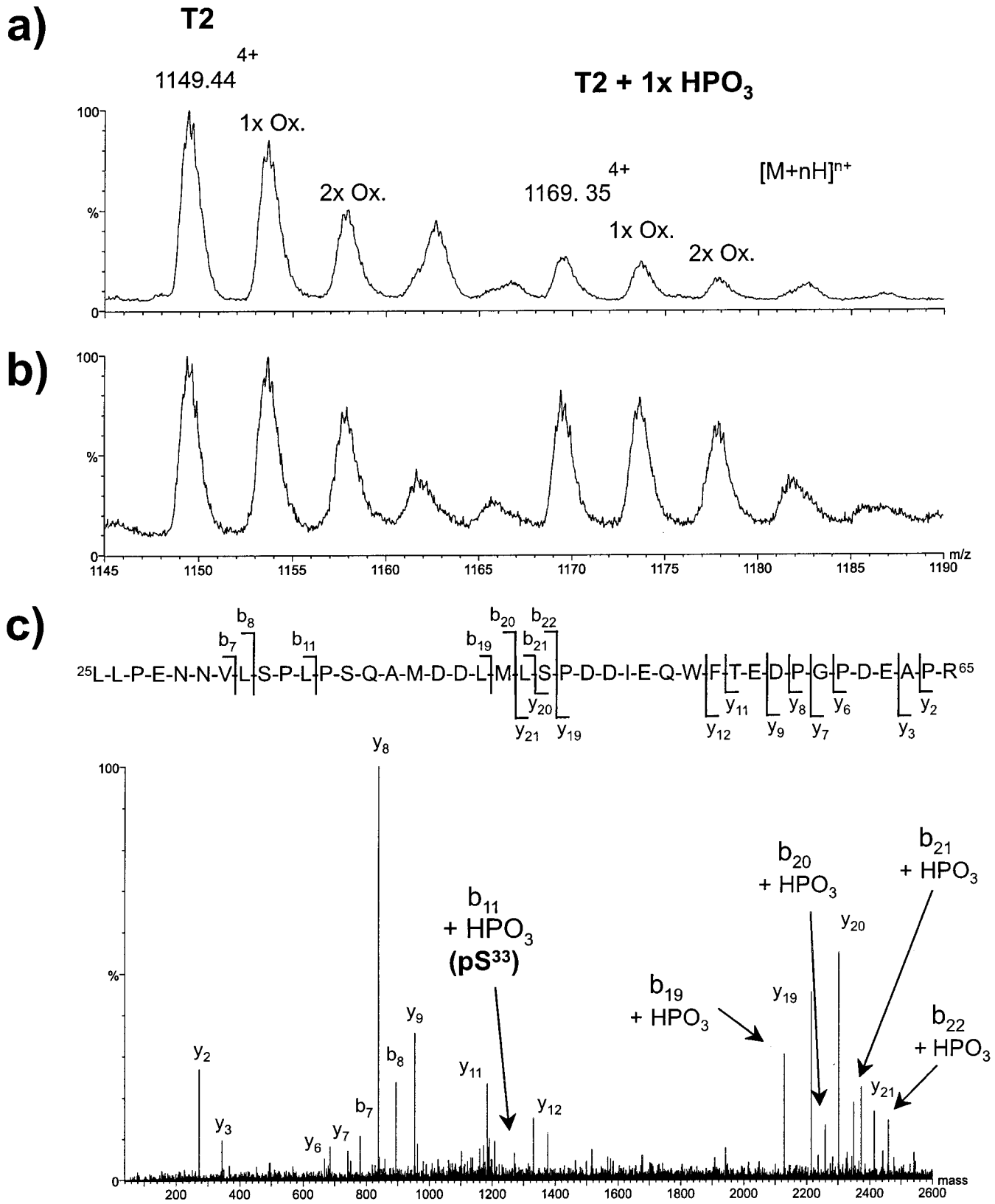

FIGURE 4: Monophosphorylation of p53$^{25-65}$ T2 peptide. Panels a and b: Total tryptic digests of control r-p53 and OA r-p53 were analyzed by LC-ESI/MS. A $(M+4H)^{+4}$ ion of *m/z* 1149.44 and related oxidized peaks (1x Ox, 2x Ox) were detected at masses corresponding to r-p53$^{25-65}$ T2 peptide (panel a). An $(M+4H)^{+4}$ of *m/z* 1169.35 was observed corresponding to monophosphorylated r-p53$^{25-65}$ T2 peptide with associated oxidized peaks. A mass spectrum of r-p53$^{25-65}$ T2 peptide from OA r-p53 showed an increase in relative intensities of the monophosphorylated T2 peak of *m/z* 1169.35 and related oxidized species when compared to the unmodified T2 *m/z* 1149.44 peak and its oxidized forms (panel b). Panel c: Phosphorylation of Ser^{33} determined by ESI/MS/MS of the *m/z* 1169.35 ion corresponding to p53$^{25-65}$ T2 peptide from panels a and b. The total tryptic digest of r-p53 was analyzed by HPLC-ESI/MS. Signals exceeding a preset intensity were collisionally activated to generate an MS/MS spectrum. Analysis of the y and b ion fragmentation series revealed the presence of a phosphoryl group at Ser^{33}, because the additional mass of the phosphoryl group occurs at the b^{11} ion and all subsequent b ions, but not immediately prior to Ser^{33}, at b^{7} and b^{8}.

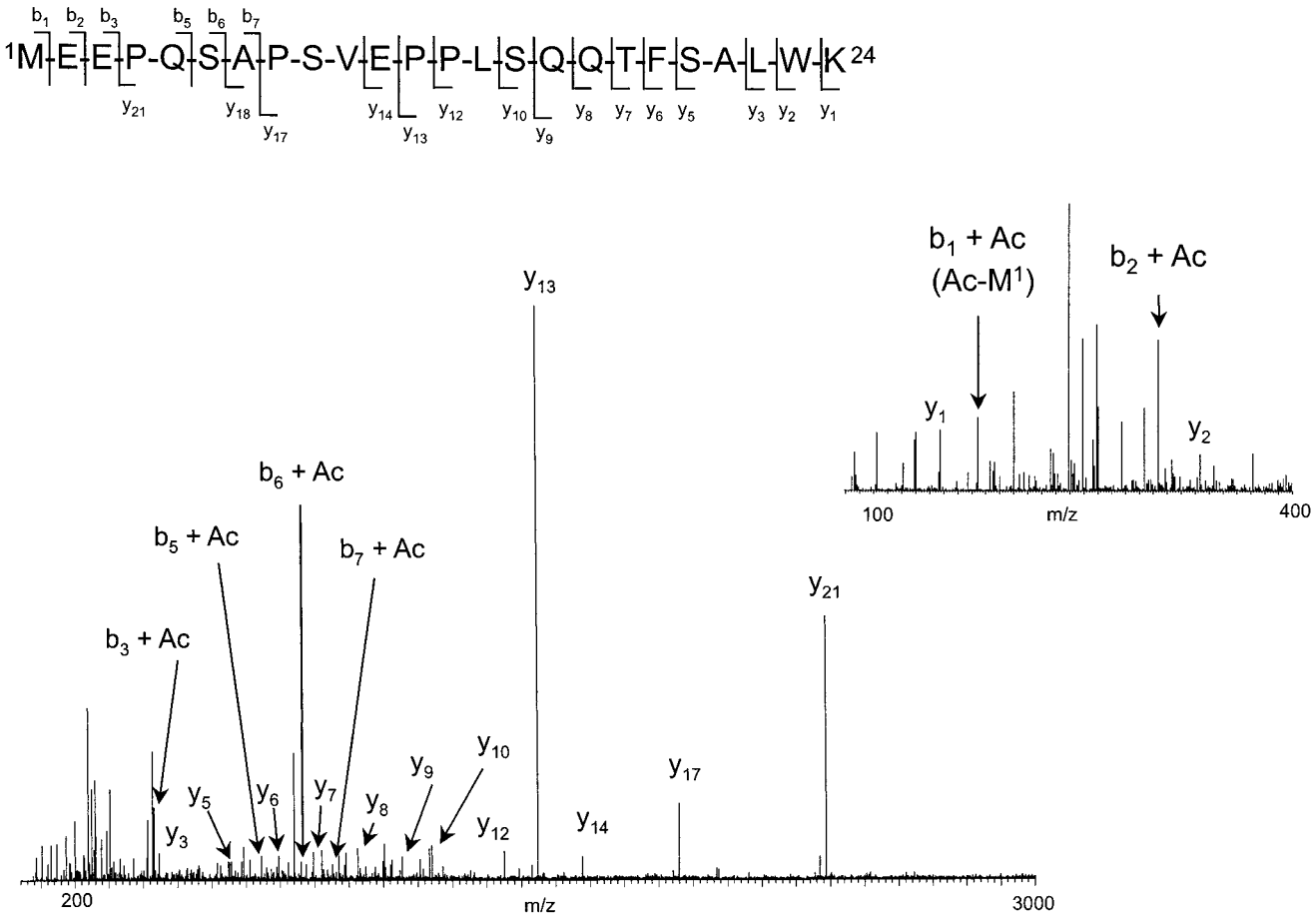

FIGURE 5: N-terminal acetylation of methionine. ESI/MS/MS of the *m*/*z* 940.5 ion corresponding to the $p53^{1-24}$ T1 peptide. Total tryptic digests of r-p53 were analyzed by HPLC-ESI/MS. Signals exceeding a preset intensity threshold were collisionally activated to generate an MS/MS spectrum. Secondary fragmentation of the $(M+3H)^{3+}$ ion of *m*/*z* 940.5 identified it as T1. The b ion fragmentation series revealed the presence of an acetylated methionine at the first ion, b_1, as indicated in an enlarged portion of the total spectrum in the upper right inset. All subsequent b ions were acetylated. The y ion series was consistent with the predicted masses of unacetylated amino acids from the carboxy terminus of the T1 peptide.

total tryptic peptide mixture without prior separation. The mass spectra of the peptide mixtures from the control r-p53 digest (Figure 2a) and OA r-p53 digest (Figure 2b) showed ion signals which could be assigned to tryptic peptides, labeled as T*x*, where *x* equals the numerical order of tryptic peptides from the amino to the carboxy terminus (Figure 3). The amino acids included in each tryptic fragment are indicated by superscripts on p53.

In these MALDI/MS analyses, peptides of total r-p53 tryptic digests covered 48% and 51% of the p53 sequence from control r-p53 and OA r-p53 proteins, respectively (Figure 3). Furthermore, ion signals which were 80 Da higher (or multiples thereof) than the calculated mass for a tryptic peptide indicated the addition of a phosphoryl group (arrows). Review of the spectrum for control r-p53 digest in Figure 2a showed an ion corresponding to the $r\text{-}p53^{25-65}$ T2 peptide (*m*/*z* 4595) and also higher ions at single and double increments of 80 Da (arrows) which suggested singly and doubly phosphorylated T2 peptides. The signal intensities of the singly and doubly phosphorylated T2 peptides dropped substantially compared to the unmodified T2 peptide. Another ion signal detected at *m*/*z* 2820 corresponded to the calculated mass for $p53^{1-24}$ T1 plus the addition of an acetyl group (labeled as T1*). An 80 Da higher ion of *m*/*z* 2900 (see Figure 2a inset) corresponded to a monophosphorylated T1* peptide.

In contrast to the MALDI/MS spectrum of the control r-p53 digest, the OA r-p53 mass spectrum in Figure 2b showed no ions corresponding to $r\text{-}p53^{25-65}$ T2, monophosphorylated T2, or diphosphorylated T2. This observation was probably due to ion suppression effects upon increased phosphorylation of T2 peptide. The MALDI/MS spectrum of the OA r-p53 digest did, however, reveal ions corresponding to the mass calculated for T1* (*m*/*z* 2820) as well as singly phosphorylated T1* (*m*/*z* 2900) and doubly phosphorylated T1* (*m*/*z* 2980). Notably, the relative peak intensity of nonphosphorylated T1* (*m*/*z* 2820) was reduced compared to control in the presence of monophosphorylated T1* at *m*/*z* 2900 and diphosphorylated T1* at *m*/*z* 2980 (Figure 2b inset). Although ion signal intensity is not absolutely quantitative, it does reflect changes in relative proportions among related ions. Overall, these MALDI/MS data suggest that there was a higher degree of phosphorylation in T1* of OA r-p53 than in T1* of control r-p53.

To confirm the assignments of the signals and to identify the phosphorylation sites, tandem mass spectrometry (MS/MS) experiments were performed using an electrospray ionization (ESI) mass spectrometer coupled with direct online liquid chromatography (LC). The online LC and MS coupling (LC-MS) has the advantage of being less susceptible to ion suppression effects, which are very common during direct mass spectrometric analysis of protein digests. In the LC-

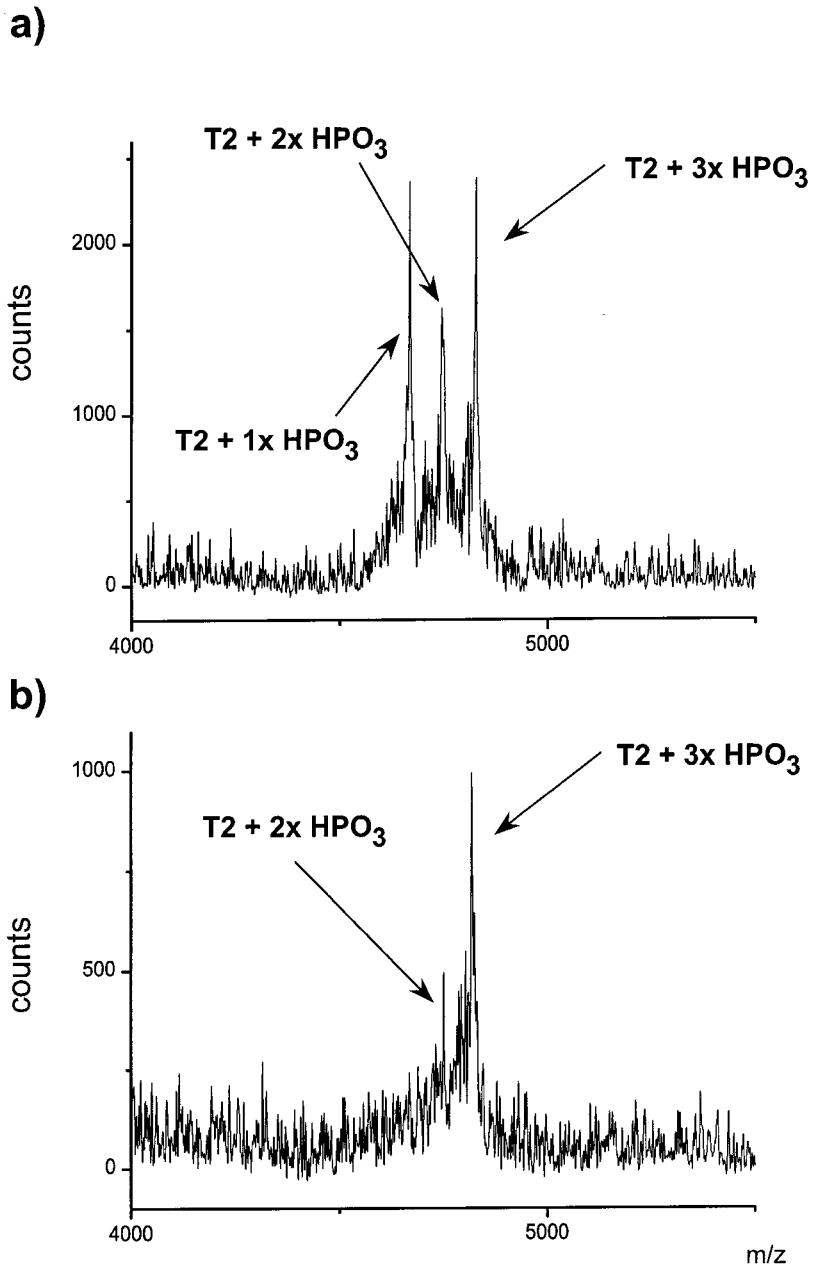

FIGURE 6: Detection of di- and triphosphopeptides of $p53^{25-65}$ T2 after Ga^{3+} affinity chromatography. The phosphopeptides in the p53 tryptic digest were affinity purified using Ga^{3+} IMAC. Ga^{3+} column retentates were analyzed directly by MALDI/MS. Peaks corresponding to mono-, di-, and triphosphorylated tryptic peptide T2 were observed from control r-p53 in panel a but were proportionately shifted to di- and triphosphorylated tryptic peptide as shown in panel b from OA r-p53 T2 retentate.

MS analysis of control r-p53, quadruply charged ion signals of *m*/*z* 1149.44 and 1169.35 were detected, which correspond to ions of tryptic peptide T2 and its monophosphorylated isoform (Figure 4a). In contrast to the MALDI/MS analysis (Figure 2a), these peptides were also detected in the LC-MS analysis of OA r-p53 (Figure 4b). Furthermore, the ratio of monophosphorylated r-$p53^{25-65}$ T2 peptide to unphosphorylated r-$p53^{25-65}$ T2 peptide is lower for the control r-p53 than for OA r-p53, indicating a higher degree of phosphorylation of r-$p53^{25-65}$ T2 peptide in OA r-p53. To identify the phosphorylation site in monophosphorylated r-$p53^{25-65}$ T2 peptide, an LC-MS/MS analysis of *m*/*z* 1169.35 was performed (Figure 4c). The LC-MS/MS spectrum shows C-terminal and N-terminal fragment ions of T2, labeled as y-ions and b-ions according to the nomenclature of Roepstorff and Fohlman (*49*). Additionally, ion signals were found that corresponded to b-ions which contain one phosphoryl group. These are labeled as $b_x + HPO_3$ where *x* indicates a particular fragmentation site. The presence of b_8 (aa 25−32) and the fragment ion $b_{11} + HPO_3$ (aa 25−35) unambiguously localized the phosphorylation site to Ser^{33}.

Furthermore, in the LC-MS analysis of control r-p53 and OA r-p-53, a triply charged ion of *m*/*z* 940.51 was observed which could be assigned to the monoacetylated r-$p53^{1-24}$ T1 peptide. An LC-MS/MS analysis of this ion confirmed this assignment, and Met^1 was unambiguously identified as the acetylated amino acid in T1 peptide (Figure 5). The phosphorylated isoforms of $p53^{1-24}$ T1 peptide, which were observed by MALDI/MS (see Figure 2), could not, however, be detected by LC-MS. The ionization efficiency of the electrospray technique depends on the proton affinity of the analyte. Neutralizing the positive charge of the amino groups

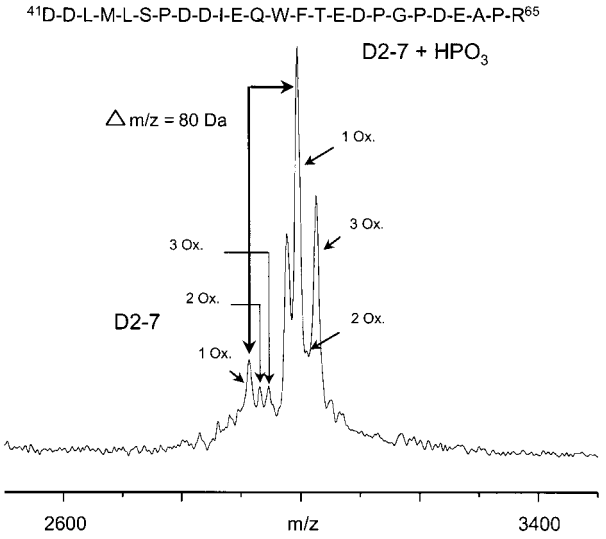

FIGURE 7: MALDI/MS of the Asp-N digestion T2 product, r-p53$^{41-65}$, shows the presence of monophosphorylation. A further enzymatic cleavage with Asp-N peptidase was performed on the HPLC-purified r-p53$^{25-65}$ T2 peptide (from control r-p53) to yield r-p53$^{41-65}$ or D2-7. Examination of the masses of the Asp-N digestion products after MALDI/MS revealed 3 oxidative states (1 Ox., 2 Ox., 3 Ox.) of an unmodified and monophosphorylated peptide.

by acetylation and incorporating negative charges by phosphorylation decrease the proton affinity of a peptide. This decrease in proton affinity, combined with the inherent acidity of r-p53$^{1-24}$ T1 peptide (predicted pI = 3.71), may be reasons for the inability to detect phosphorylated T1* peptide by ESI/MS.

For selective and specific identification of multiply phosphorylated peptides, the combination of IMAC using Ga^{3+} with direct MALDI/MS analysis was applied (*46*). In Figure 6, the MALDI/MS spectra of the control r-p53 digest and the OA r-p53 digest obtained after IMAC of the tryptic peptide mixture are shown. The MALDI mass spectrum of the control r-p53 digest demonstrated that r-p53$^{25-65}$ T2 peptide is singly, doubly, and triply phosphorylated, and that the corresponding ion signals occur in a ratio of 1:0.5:1 (Figure 6a). The MALDI mass spectrum of the OA r-p53 digest contained ions corresponding to diphosphorylated T2 peptide and the triphosphorylated T2 peptide, with the triply phosphorylated peptide being the most abundant (Figure 6b). No significant ion signal corresponding to monophosphorylated r-p53$^{25-65}$ T2 peptide was observed for OA r-p53 digests.

To localize the two additional phosphorylation sites on r-p53$^{25-65}$ T2 peptide, the T2 peptides were separated from the other tryptic p53 peptides by HPLC. The isolated peptides were then proteolytically digested with Asp-N, and analyzed by MALDI/MS. The MALDI mass spectrum contained signals corresponding to D2−7 (aa 41−65) and a monophosphorylated form (Figure 7). The r-p53$^{25-65}$ T2 peptide contained a total of four possible phosphorylation sites, but the data in Figure 6 indicated that only three of these sites were phosphorylated. The monophosphorylation of the D2−7 digestion product was revealing because only one of the phosphorylation sites on D2−7 was occupied, suggesting that the remaining other two phosphorylation sites must have been Ser^{33} (confirmed by ESI/MS/MS) and Ser^{37}. Of the two possible phosphorylation sites (Ser^{46} or Thr^{55}) on the r-p53$^{41-65}$ D2−7 peptide, Ser^{46} is a likely choice because it corresponds to an -SP- proline-directed kinase sequence while the sequence surrounding Thr^{55} does not contain a recognizable kinase motif.

Serine^{315} Is Completely Phosphorylated in OA r-p53 Compared to a Minimum in Control r-p53. The MALDI mass spectrum of the HPLC-separated tryptic peptides from r-p53 contained ions corresponding to the tryptic peptide, r-p53$^{307-319}$ T30, and its monophosphorylated isoform, which were not observed in the MALDI mass spectrum of the digest mixture. Because r-p53$^{307-319}$ T30 contains four potential phosphorylation sites, tandem mass spectrometry was applied to verify the phosphorylation site at Ser^{315} (*50*). Figure 8 shows the ESI/MS spectra of r-p53$^{307-319}$ T30 from control r-p53 (Figure 8a) and from OA r-p53 (Figure 8b). In the OA r-p53, r-p53$^{307-319}$ T30 is completely monophosphorylated, whereas r-p53$^{307-319}$ T30 in the control r-p53 spectrum shows only 5% phosphorylation. This is based on the intensity difference between the corresponding ion signals of nonphosphorylated vs monophosphorylated r-p53$^{307-319}$ T30 in control r-p53. Ser^{315} was unambiguously identified as the phosphorylation site in monophosphorylated r-p53$^{307-319}$ T30 by observation of the fragment ions y_4 (aa 319−316) and $y_5 + HPO_3$ (aa 319−315) in the ESI/MS/MS spectrum (Figure 8c). The presence of b_7 and b_8 ions indicates that only Ser^{315} is phosphorylated.

Biochemical studies were carried out to determine if the Ser^{315} site was phosphosaturated in the OA r-p53 as suggested by MS data in Figure 8. Since Ser^{315} is a CDK2 kinase specific site (*50*), control r-p53 and OA r-p53 served as substrates in a human CDK2 *in vitro* kinase assay (Figure 9: top panel, lanes 1−4). Compared to a robust CDK2 kinase activity with control r-p53 (lane 1), it is clear that little additional phosphorylation occurs with hyperphosphorylated r-p53 after OA treatment (lane 3), after accounting for nonspecific kinase activity attached to agarose beads (lanes 2 and 4). The bar graph of relative kinase activity after phosphorimaging shows a comparable amount of phosphorylation (7−15% of control r-p53) among the OA p53 and nonspecific kinase activities. These biochemical observations suggest that OA r-p53 cannot be further phosphorylated by CDK2 kinase.

Because control r-p53 served as an excellent CDK2 kinase substrate, it was of interest to separate the control r-p53 labeled by ^{32}P with CDK2 by 2D PAGE since isoelectric focusing would reveal if labeling r-p53 at one site (Ser^{315}) would produce one or multiple phosphoisoforms. The inset to the control r-p53 in Figure 9 clearly shows five well-resolved ^{32}P-labeled isoforms (arrows). Isoelectric focusing of control r-p53 labeled by nonspecific kinases (see inset below "N.S." without arrows) also showed several phosphoisoforms of lesser intensity and resolution than by CDK2 kinase. Isoelectric focusing of ^{32}P-labeled OA r-p53 from lanes 3 and 4 produced low intensity, poorly resolved isoforms (data not shown) comparable to N.S. isoforms for control r-p53. Western blotting of ^{32}P-labeled isoforms confirmed they were p53 proteins and gave a corresponding pattern (data not shown).

DISCUSSION

Various stressors activate kinases and phosphatases in signaling pathways that modify p53 from its basal phospho-

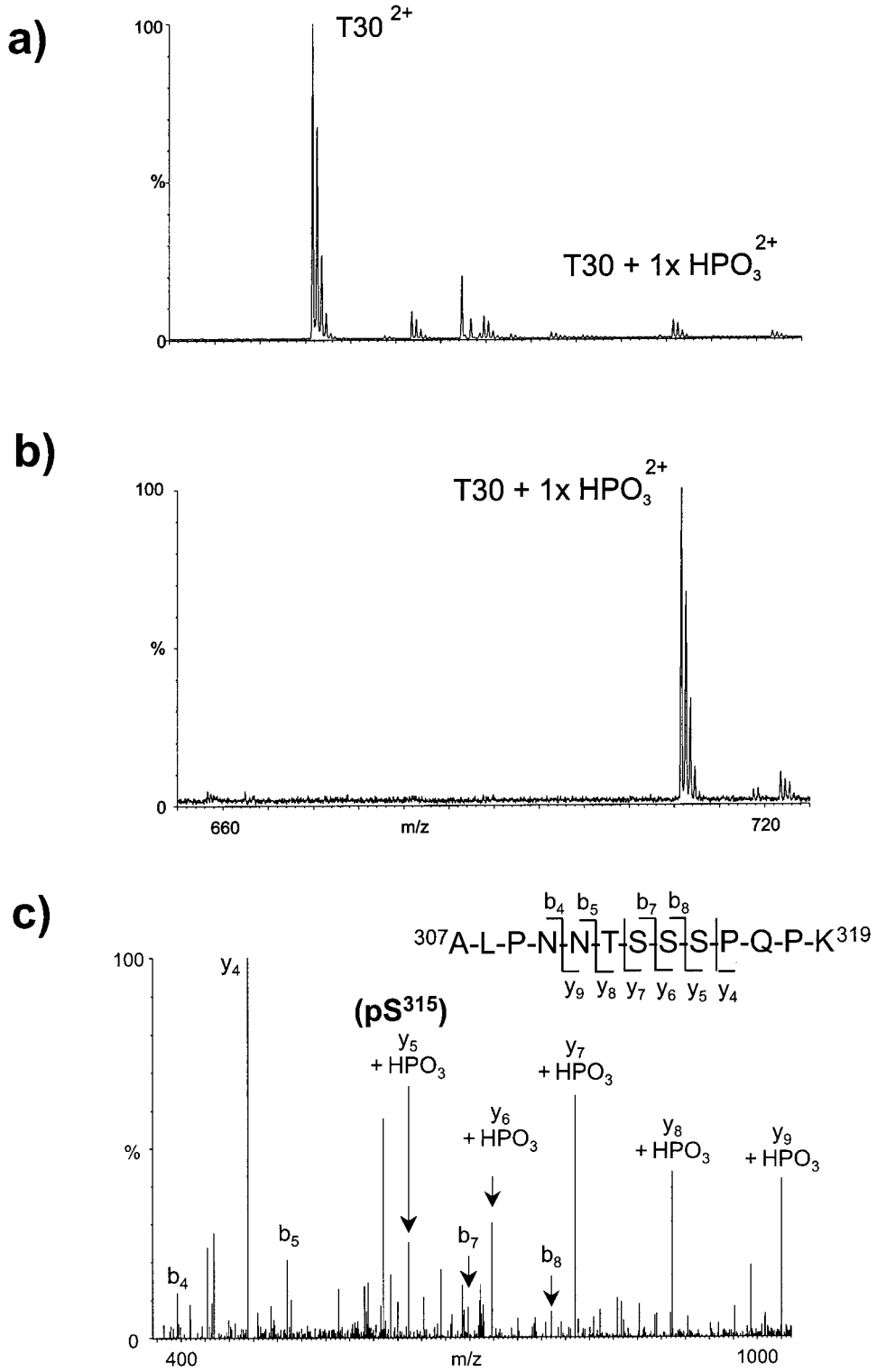

FIGURE 8: Saturating phosphorylation of Ser^{315} by okadaic acid treatment. Panels a and b: The r-p53$^{307-319}$ T30 peptide was HPLC purified offline from total tryptic digests of control r-p53 and OA r-p53, and then reanalyzed by nanoflow ESI/MS. The mass spectrum of HPLC-purified T30 in the upper scan for control r-p53 shows the majority of signal at *m*/*z* 711 $(M+2H)^{2+}$ and only a small peak at *m*/*z* 751 $(M+2H)^{2+}$ representing monophosphorylated T30. The lower scan for OA r-p53 shows almost all the signal from HPLC-purified T30 resides in the monophosphorylated peak. Panel c: Phosphorylation of Ser^{315} determined by ESI/MS/MS of peak 710.8 corresponding to the phosphorylated tryptic peptide, T30. Fragmentation of ions *m*/*z* 710.8 produced a y ion series which revealed the addition of a phosphate at the y^5 and subsequent y ions, indicating phosphorylation at Ser^{315}.

rylated state to a stabilized and activated form capable of regulating cell growth, survival, or death. In this study, we used the baculovirus expression system in sf9 cells as a model system to determine p53 phosphorylation sites by mass spectrometry. A 48 h expression period under control conditions produced a basal level of phosphorylation (*40*) which was compared to hyperphosphorylated species of r-p53 reported for okadaic acid exposure (*43*). We verified the effect of okadaic acid biochemically by observing an acidic shift of phosphoisoforms after isoelectric focusing which

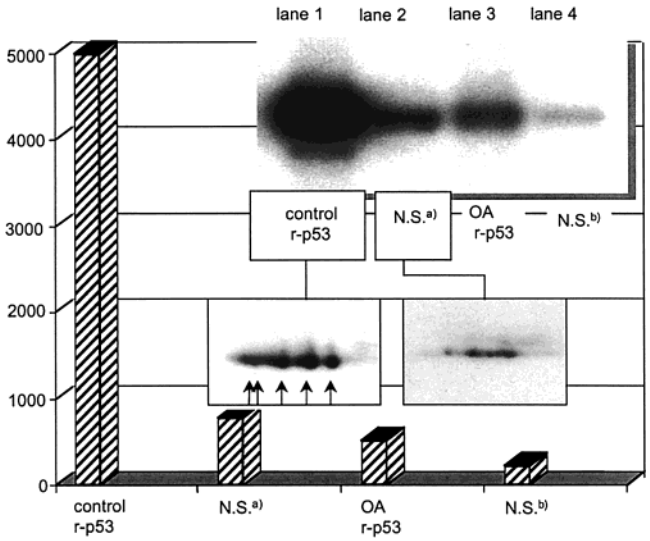

FIGURE 9: Biochemical validation of saturating phosphorylation at Ser[315]. Control r-p53 and OA r-p53 were compared as CDK2 kinase substrates in an *in vitro* kinase assay. CDK2 kinase from immunoprecipitants of 200 μg of human cell lysate was used for each reaction. CDK2 specifically phosphorylates p53 at Ser[315] *in vitro* as shown by the autoradiograph in the upper right inset. Lane 1 is ^{32}P-labeled control r-p53 phosphorylated in the presence of CDK2; lane 2 is ^{32}P-labeled control r-p53 which was radiolabeled in the absence of CDK2 and shows background labeling by nonspecific (N.S.) kinases. Lane 3 is ^{32}P-labeled OA r-p53 phosphorylated in the presence of CDK2; lane 4 is ^{32}P-labeled OA r-p53 which is radiolabeled in the absence of CDK2 and shows background labeling by nonspecific (N.S.) kinases. Bands in the upper right inset were quantitated by phosphorimage analysis. Phosphorylation intensities are displayed in the bar graph in cumulative gray values (y axis = arbitrary units). Comparable portions of CDK2 kinase labeled control r-p53 and the negative control were separated into phosphoisoforms by 2D PAGE analysis as shown by the boxed insets. Five phosphoisoforms were detected by autoradiography as shown by arrows in the control r-p53 boxed inset. 2D PAGE separation of nonspecifically labeled control r-p53 was of lesser intensity and resolution by comparison.

indicates increased phosphorylation (*51, 52*). In addition, the greater mass of OA r-p53 over control r-p53, indicated by a mean 214 Da mass increase, represented either a 2.7-fold net rise in phosphorylation or a mass gain from other posttranslational groups. Our intent was to determine phosphorylation sites during basal expression of p53 and to examine the action of okadaic acid either in saturating basal phosphorylation sites or in eliciting new phosphorylation sites and other modifications.

We used several approaches for separation and MS analysis to determine the phosphorylation status of p53. In this study, we found modifications on three primary tryptic fragments of p53. The first 2 tryptic fragments, p53$^{1-24}$ T1 peptide and p53$^{25-65}$ T2 peptide, span the initial 65 amino acids in the important N-terminal region while the tryptic fragment, r-p53$^{307-319}$ T30 peptide, contained a CDK2 site. MALDI/MS of total tryptic digests of r-p53 produced an ion spectrum for which tryptic fragments matched about 50% of the entire p53 sequence. The MALDI/MS analysis, however, indicated the presence of phosphopeptides in only two fragments from the N-terminus: in p53$^{1-24}$ T1 peptide from both control and OA r-p53 digests and only in p53$^{25-65}$ T2 peptide from the control p53 digest. Importantly, no ion could be detected in tryptic digests by MALDI-MS for the p53$^{307-319}$ T30 peptide containing the CDK2 site at Ser[315]. Ion suppression may have contributed to the inability to detect any p53$^{307-319}$ T30 peptide and may also explain the absence of phosphorylated p53$^{25-65}$ T2 peptide ion signal from OA r-p53 digests. A combination of factors including proportionally small levels of phosphorylation and ion suppression effects make detection of phosphopeptides in tryptic digests challenging.

Immobilized metal affinity chromatography (IMAC) with Ga^{3+} provided a means to exploit gallium's selectivity for phosphopeptides as demonstrated by the Tempst lab (*47*) and in this lab (*46*). Ga^{3+} IMAC enrichment of r-p53 tryptic digests and analysis by MALDI/MS showed the presence of three phosphorylations on the p53$^{25-65}$ T2 peptide whereas ESI/MS/MS detected one site on the T2 peptide. Furthermore, mono-, di-, and triphosphopeptides of p53$^{25-65}$ peptide under basal conditions were shifted to primarily di- and triphosphopeptides by okadaic acid treatment. While the intensities of the MALDI/MS signals were not expected to directly correlate to r-p53 levels, the basal and hyperphosphorylated r-p53 preparations could be distinguished from MS data. Thus, Ga^{3+} IMAC was able to concentrate multiphosphorylated peptides for detection by MALDI/MS whereas their presence was previously suppressed in whole tryptic digests.

MS/MS spectra positively identified N-terminal acetylation and phosphorylation at Ser[33] and Ser[315] in this study. Many proteins are N-terminal-acetylated (*53*) if any of the adjacent amino acids belong to the DEN subgroup (Asp, Glu, or Asn) as does p53 (Glu[2], Glu[3]), and this modification may serve as a prophylactic cap to prevent premature or inappropriate degradation of newly synthesized proteins (*54*). Assignment of phosphorylation at Ser[37] and Ser[46] (*25*) was deduced from MALDI/MS data after IMAC purification and from Asp-N digestion of the p53$^{25-65}$ T2 peptide. In addition, we found two phosphorylations on the p53$^{1-24}$ T1 peptide after okadaic acid treatment which probably reflect phosphorylations at Thr[18] and Ser[20] as recently found from baculovirus r-p53 by site-specific, anti-phospho-antibodies (*24*). The power of MS to find novel phosphorylation sites is exemplified by Ser[46]. A recent study found that a new phosphorylation site, Ser[46], as well as Ser[33] were both phosphorylated using a synthetic p53$^{25-65}$ peptide which was phosphorylated *in vitro* by UV radiation-activated p38 kinase (*25*). Even more convincing is recent evidence that a new gene, p53*AIP1* or p53-regulated apoptosis-inducing protein 1, is inducible after Ser[46] phosphorylation on p53 after severe DNA damage as detected by a specific anti-phosphoserine antibody (*55*). Whether or not sf9 cells contain an equivalent to Ser[46] kinase is not yet known.

While preparing this paper, a study appeared reporting one phosphorylation at Ser[315] of wt p53 tryptic digests isolated from human OCI/AML-3 cells under control conditions (*56*). After γ-irradiation, MALDI/MS detected two phosphorylations on acetylated p53$^{1-24}$ peptide and one phosphorylation on p53$^{25-65}$ peptide. By comparison, the greater number of N-terminal phosphorylation sites found in our study on N-terminal fragments probably results from differences in sample preparation, separation, and enrichment schemes, and intensive use of tandem MS. Although the *in vitro* peptide kinase experiments indicate that many p53 phosphorylations are possible, many of these sites have not been verified. We

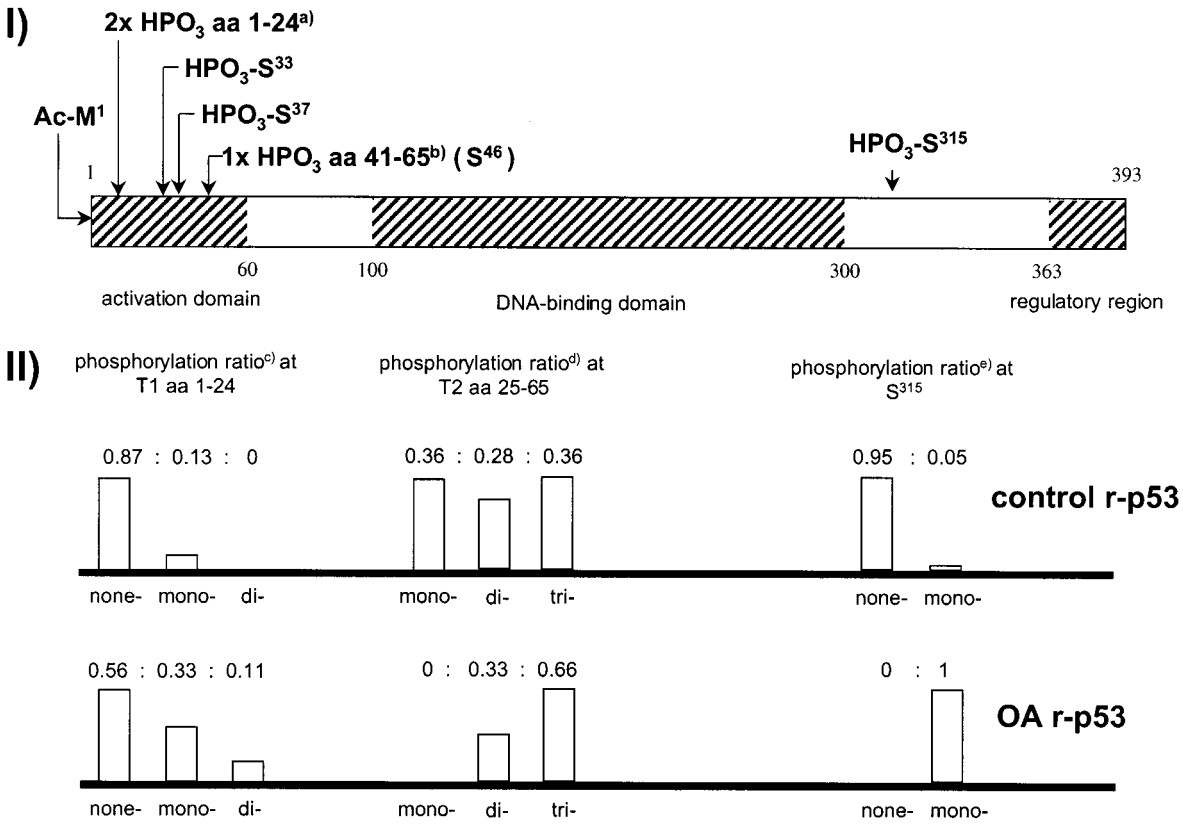

FIGURE 10: Summary of analytical results for site-specific phosphorylation of p53. Panel I: Posttranslational groups identified in this study are indicated by arrows on a domain map of p53 at the top of the figure as follows: N-terminal acetylation and two phosphorylations on $p53^{1-24}$ T1 peptide; Ser^{33}, Ser^{37}, and Ser^{46} on $p53^{25-65}$ T2 peptide; and Ser^{315} on $p53^{307-319}$ T30 peptide. The lower portion of the figure shows proportional increases at phosphorylation sites within T1, T2, and T30 peptides of r-p53 produced by okadaic acid in the sf9 baculovirus expression system. [a]Diphosphorylation (2x HPO_3) of r-$p53^{1-24}$ T1 peptide was detected although the exact sites were not determined. [b]One phosphorylation site on r-$p53^{41-65}$, the Asp-N T2 digestion product (see Figure 7), was deduced to be Ser^{46} as a proline-directed kinase site. Relative isoform proportions (equal to 1) were based on cumulative MS peak heights for each peptide in control or OA samples. [c]The intensities of ion signals observed in Figure 2 (insets of panels a and b) were used to determine the relative proportion of $p53^{1-24}$ T1 phosphopeptides. [d]Data in Figure 6 (panels a and b) were used to calculate the relative proportion of $p53^{24-65}$ T2 peptide. [e]Data in Figure 8 (panels a and b) were used to determine the relative proportion of nonphosphorylated and monophosphorylated $p53^{307-319}$ T30 peptide.

demonstrate that the correspondence between the number of p53 isoforms (six) after Western blot and the six phosphorylation sites identified by MS is evidence of the major phosphorylations under these baculovirus expression conditions. Other minor phosphorylation sites *may* occur, possibly at the carboxy terminus (*43, 57*) in addition to Ser^{315}. Furthermore, a small degree of peptide oxidation (Figures 4 and 7) was noted during p53 phosphopeptide analysis. Although some oxidation might be expected during purification and digestion procedures, the portion due to oxidation of p53 *in vivo* as a byproduct of metabolic processes or as a sign of oxidative stress is not clear but may be important in light of recent reports of tryosine nitrosylation of p53 associated with cellular redox signaling (*58*) and pathogenesis (*59*).

The pharmacological action of okadaic acid as an inhibitor of PP2A and PP1 is particularly useful in insect expression systems because the phosphorylation state of expressed p53 is primarily affected by a high phosphatase activity (*43*). Fuchs et al. (*43*) found that some serines in the N-terminus of baculovirus-expressed rat p53 were only phosphorylated in peptide mapping studies when endogenous phosphatases were inhibited by OA, suggesting the level of phosphorylation was determined by high phosphatase activity rather than unfavorable kinase:substrate ratios. In our study, OA treatment produced a second phosphorylation in the r-$p53^{1-24}$ T1 peptide that was not observed in controls and also produced higher phosphorylation ratios in r-$p53^{25-65}$ T2 peptide and r-$p53^{307-319}$ T30 phosphopeptides as summarized in Figure 10. The identified increases in phosphorylation produced by OA over control (Figure 10) probably comprise much of the increased mass of OA r-p53 initially measured by MALDI/MS prior to tryptic digestion.

Although OA efficiently increased the phosphorylation content of expressed p53 in insect cells, phosphatase inhibition by OA is not without biological consequences. In our study even with a relatively low concentration of OA at 25 nM, treatment for $\geq$24 h was toxic to insect cells, which was the reason we selected a 12 h treatment that produced comparable cell viability to untreated controls. OA is a known mitogen, causing phosphorylation and activation of the MAP kinase pathway (*60*), and has promoter activity in animals (*61*). The role that p53 phosphorylation plays in OA-mediated mitogenesis and promotion is not completely clear but may be related to selection of cells with defects in cell cycle arrest and apoptosis and upregulation of growth promotion genes (*62*). In our study, the most notable action of OA on p53 was a complete phosphorylation at Ser^{315}. Earlier work by Wang and Prives (*22*) demonstrated the importance of this site by reporting that DNA binding of p53 among different target promoters was selectively stimulated by Ser^{315} phosphorylation. Phosphorylation of Ser^{315}

may, therefore, be a critical molecular event in determining biological effects of OA.

The separation of p53 protein by isoelectric focusing produces a variable number of phosphoisoforms for a particular cell type, tissue or species (*63*, *64*). A change in the number or in the relative migration of p53 phosphoisoforms has often been used as a barometer of overall cellular p53 phosphorylation status (*39*, *51*, *65*). In our study, the action of okadaic acid in inhibiting protein phosphatase permitted detection of two more acidic p53 phosphoisoforms in addition to the four isoforms observed in control Western blots. To the extent that inhibition of protein phosphatases permits phosphorylation at an existing site to become greater or allows low-level phosphorylation to become detectable, MS data from our study suggest OA did produce a greater amount of phosphorylation at existing sites, such as Ser^{315}, as well as detect the new appearance of a second phosphorylation on T1 $p53^{1-24}$ peptide. We cannot currently assign posttranslational identities by MS analysis to each individual isoform within the 2D PAGE pattern, but our eventual attainment of this capability will permit an accurate global assessment of p53 phosphorylation status.

Whether or not a specific biological function and absolute structural identity can be assigned to each individual p53 phosphoisoform remains an important but unanswered question. For example, Mukhopadhyay et al. (*65*) found five phosphoisoforms by Western blotting in wt p53 transfected H1299 cells under basal conditions whose number was highly increased by nine more acidic isoforms after treatment with apoptotic-inducing chemicals such as vinblastine and actinomycin D. Is it likely that each isoform has a specific cellular function as they suggest? We do not believe so because each individual p53 isoform in the 2D PAGE pattern could represent a mixture of structurally distinct p53 isoforms with differing phosphorylated or acetylated sites containing the same net charge. Our observation that CDK2-mediated phosphorylation of control r-p53 at Ser^{315} produces five separable isoforms suggests that each isoform is not homogeneous. Instead we speculate that multiple isoforms serve as precursors for a distinct subpopulation(s) possessing biological activity. Further, the order in which each kinase modifies p53 may leave a signature pattern which could be reassembled by a site-specific analysis of each isoform, and which may vary in different cell types. Analysis of individual isoforms by MS, complemented by use of phosphospecific antibodies, may illuminate the manner in which different cell types adjust the function of p53.

REFERENCES

1. Lakin, N. D., and Jackson, S. P. (1999) *Oncogene 18*, 7644−7655.
2. Sakaguchi, K., Herrera, J. E., Saito, S., Miki, T., Bustin, M., Vassilev, A., Anderson, C. W., and Appella, E. (1998) *Genes Dev. 12*, 2831−2841.
3. Shieh, S. Y., Ikeda, M., Taya, Y., and Prives, C. (1997) *Cell 91*, 325−334.
4. Shieh, S. Y., Taya, Y., and Prives, C. (1999) *EMBO J. 18*, 1815−1823.
5. Siliciano, J. D., Canman, C. E., Taya, Y., Sakaguchi, K., Appella, E., and Kastan, M. B. (1997) *Genes Dev. 11*, 3471−3481.
6. Fuchs, S. Y., Adler, V., Buschmann, T., Yin, Z., Wu, X., Jones, S. N., and Ronai, Z. (1998) *Genes Dev. 12*, 2658−2663.
7. Fuchs, S. Y., Adler, V., Buschmann, T., Wu, X., and Ronai, Z. (1998) *Oncogene 17*, 2543−2547.
8. Tao, W., and Levine, A. J. (1999) *Proc. Natl. Acad. Sci. U.S.A. 96*, 3077−3080.
9. Freedman, D. A., Wu, L., and Levine, A. J. (1999) *Cell Mol. Life Sci. 55*, 96−107.
10. Dobbelstein, M., Wienzek, S., Konig, C., and Roth, J. (1999) *Oncogene 18*, 2101−2106.
11. Lakin, N. D., Hann, B. C., and Jackson, S. P. (1999) *Oncogene 18*, 3989−3995.
12. Chehab, N. H., Malikzay, A., Appel, M., and Halazonetis, T. D. (2000) *Genes Dev. 14*, 278−288.
13. Dumaz, N., Milne, D. M., and Meek, D. W. (1999) *FEBS Lett. 463*, 312−316.
14. Khosravi, R., Maya, R., Gottlieb, T., Oren, M., Shiloh, Y., and Shkedy, D. (1999) *Proc. Natl. Acad. Sci. U.S.A. 96*, 14973−14977.
15. Lees-Miller, S. P., Sakaguchi, K., Ullrich, S. J., Appella, E., and Anderson, C. W. (1992) *Mol. Cell. Biol. 12*, 5041−5049.
16. Tibbetts, R. S., Brumbaugh, K. M., Williams, J. M., Sarkaria, J. N., Cliby, W. A., Shieh, S. Y., Taya, Y., Prives, C., and Abraham, R. T. (1999) *Genes Dev. 13*, 152−157.
17. Ko, L. J., Shieh, S. Y., Chen, X., Jayaraman, L., Tamai, K., Taya, Y., Prives, C., and Pan, Z. Q. (1997) *Mol. Cell. Biol. 17*, 7220−7229.
18. Liu, J. P. (1999) *FASEB J. 13*, 2091−2104.
19. Hupp, T. R., and Lane, D. P. (1994) *Cold Spring Harb. Symp. Quant. Biol. 59*, 195−206.
20. Cuddihy, A. R., Wong, A. H., Tam, N. W., Li, S., and Koromilas, A. E. (1999) *Oncogene 18*, 2690−2702.
21. Takenaka, I., Morin, F., Seizinger, B. R., and Kley, N. (1995) *J. Biol. Chem. 270*, 5405−5411.
22. Wang, Y., and Prives, C. (1995) *Nature 376*, 88−91.
23. Waterman, M. J., Stavridi, E. S., Waterman, J. L., and Halazonetis, T. D. (1998) *Nat. Genet. 19*, 175−178.
24. Craig, A. L., Burch, L., Vojtesek, B., Mikutowska, J., Thompson, A., and Hupp, T. R. (1999) *Biochem. J. 342*, 133−141.
25. Bulavin, D. V., Saito, S., Hollander, M. C., Sakaguchi, K., Anderson, C. W., Appella, E., and Fornace, A. J., Jr. (1999) *EMBO J. 18*, 6845−6854.
26. Kapoor, M., and Lozano, G. (1998) *Proc. Natl. Acad. Sci. U.S.A. 95*, 2834−2847.
27. Bond, J. A., Webley, K., Wyllie, F. S., Jones, C. J., Craig, A., Hupp, T., and Wynford-Thomas, D. (1999) *Oncogene 18*, 3788−3792.
28. Blattner, C., Tobiasch, E., Litfen, M., Rahmsdorf, H. J., and Herrlich, P. (1999) *Oncogene 18*, 1723−1732.
29. Ashcroft, M., Kubbutat, M. H., and Vousden, K. H. (1999) *Mol. Cell. Biol. 19*, 1751−1758.
30. Simbulan-Rosenthal, C. M., Rosenthal, D. S., Luo, R., and Smulson, M. E. (1999) *Cancer Res. 59*, 2190−2194.
31. Smith, H. M., and Grosovsky, A. J. (1999) *Carcinogenesis 20*, 1439−1443.
32. Shaw, P., Freeman, J., Bovey, R., and Iggo, R. (1996) *Oncogene 12*, 921−930.
33. Rodriguez, M. S., Desterro, J. M., Lain, S., Midgley, C. A., Lane, D. P., and Hay, R. T. (1999) *EMBO J. 18*, 6455−6461.
34. Otvos, L., Jr., Hoffmann, R., Xiang, Z. Q., O, I., Deng, H., Wysocka, M., Pease, A. M., Rogers, M. E., Blaszczyk-Thurin, M., and Ertl, H. C. (1998) *Biochim. Biophys. Acta 1404*, 457−474.
35. Chong, B. E., Lubman, D. M., Rosenspire, A., and Miller, F. (1998) *Rapid Commun. Mass Spectrom. 12*, 1986−1993.
36. Fuchs, B., O'Connor, D., Fallis, L., Scheidtmann, K. H., and Lu, X. (1995) *Oncogene 10*, 789−793.
37. Hecker, D., Page, G., Lohrum, M., Weiland, S., and Scheidtmann, K. H. (1996) *Oncogene 12*, 953−961.
38. Martone, T., Airoldi, L., Magagnotti, C., Coda, R., Randone, D., Malaveille, C., Avanzi, G., Merletti, F., Hautefeuille, A., and Vineis, P. (1998) *Int. J. Cancer 75*, 512−516.
39. Merrick, B. A., Pence, P. M., He, C., Patterson, R. M., and Selkirk, J. K. (1995) *BioTechniques 18*, 292−299.

40. Patterson, R. M., He, C., Selkirk, J. K., and Merrick, B. A. (1996) *Arch. Biochem. Biophys. 330*, 71−79.
41. Zhang, W., McClain, C., Gau, J. P., Guo, X. Y., and Deisseroth, A. B. (1994) *Cancer Res. 54*, 4448−4453.
42. Yatsunami, J., Komori, A., Ohta, T., Suganuma, M., and Fujiki, H. (1993) *Cancer Res. 53*, 239−241.
43. Fuchs, B., Hecker, D., and Scheidtmann, K. H. (1995) *Eur. J. Biochem. 228*, 625−639.
44. Stenger, J. E., Mayr, G. A., Mann, K., and Tegtmeyer, P. (1992) *Mol. Carcinog. 5*, 102−106.
45. Frank, A. W. (1984) *CRC Crit. Rev. Biochem. 16*, 51−101.
46. Zhou, W., Merrick, B. A., Khaledi, M. G., and Tomer, K. B. (2000) *J. Am. Soc. Mass Spectrom. 11*, 273−282.
47. Posewitz, M. C., and Tempst, P. (1999) *Anal. Chem. 71*, 2883−2892.
48. Hitomi, M., Shu, J., Strom, D., Hiebert, S. W., Harter, M. L., and Stacey, D. W. (1996) *J. Biol. Chem. 271*, 9376−9383.
49. Roepstorff, P., and Fohlman, J. (1984) *Biomed. Mass Spectrom. 11*, 601.
50. Price, B. D., Hughes-Davies, L., and Park, S. J. (1995) *Oncogene 11*, 73−80.
51. Ullrich, S. J., Mercer, W. E., and Appella, E. (1992) *Oncogene 7*, 1635−1643.
52. Guy, G. R., Philp, R., and Tan, Y. H. (1995) *Eur. J. Biochem. 229*, 503−511.
53. Bradshaw, R. A., Brickey, W. W., and Walker, K. W. (1998) *Trends Biochem. Sci. 23*, 263−267.
54. Varshavsky, A. (1996) *Proc. Natl. Acad. Sci. U.S.A. 93*, 12142−12149.
55. Oda, K., Arakawa, H., Tanaka, T., Matsuda, K., Tanikawa, C., Mori, T., Nishimori, H., Tamai, K., Tokino, T., Nakamura, Y., and Taya, Y. (2000) *Cell 102*, 849−862.
56. Abraham, J., Kelly, J., Thibault, P., and Benchimol, S. (2000) *J. Mol. Biol. 295*, 853−864.
57. Mundt, M., Hupp, T., Fritsche, M., Merkle, C., Hansen, S., Lane, D., and Groner, B. (1997) *Oncogene 15*, 237−244.
58. Marshall, H. E., Merchant, K., and Stamler, J. S. (2000) *FASEB J. 14*, 1889−1900.
59. Kolb, J. P. (2000) *Leukemia 14*, 1685−1694.
60. Rossini, G. P., Pinna, C., and Malaguti, C. (1999) *Biochem. Pharmacol. 58*, 279−284.
61. Fujiki, H. (1992) *Mol. Carcinog. 5*, 91−94.
62. Milczarek, G. J., Chen, W., Gupta, A., Martinez, J. D., and Bowden, G. T. (1999) *Carcinogenesis 20*, 1043−1048.
63. Milczarek, G. J., Martinez, J., and Bowden, G. T. (1997) *Life Sci. 60*, 1−11.
64. Prives, C., and Hall, P. A. (1999) *J. Pathol. 187*, 112−126.
65. Mukhopadhyay, T., Roth, J. A., Acosta, S. A., and Maxwell, S. A. (1998) *Apoptosis 3*, 421−430.

BI002045I